

Slow Passage through a Saddle-Center Bifurcation

D. C. Diminnie¹ and R. Haberman²

Department of Mathematics, Southern Methodist University, Dallas, TX 75275, USA

Received September 24, 1998; accepted August 9, 1999

Communicated by Stephen Wiggins

Summary. Slowly varying conservative one-degree of freedom Hamiltonian systems are analyzed in the case of a saddle-center bifurcation. Away from unperturbed homoclinic orbits, strongly nonlinear oscillations are obtained using the method of averaging. A long sequence of nearly homoclinic orbits is matched to the strongly nonlinear oscillations before and after the slow passage. Usually solutions pass through the separatrix associated with the double homoclinic orbit before the saddle-center bifurcation occurs. For the case of slow passage through the special homoclinic orbit associated with a saddle-center bifurcation, solutions consist of a large sequence of nearly saddle-center homoclinic orbits connecting autonomous nonlinear saddle approaches, and the change in the action is computed. However, if the energy at one specific saddle approach is particularly small, then that one nonlinear saddle approach instead satisfies the nonautonomous first Painlevé transcendent, in which case the solution usually either passes through the saddle-center homoclinic orbit in nearly the same way or makes a transition backwards in time to small oscillations around the stable center (though it is possible that the solution approaches the unstable saddle).

Key words. saddle-center bifurcation, passage through a separatrix, homoclinic orbits, averaging, change in action, nonlinear saddle point, nonautonomous saddle approach, first Painlevé transcendent, generalized Riemann zeta function, slowly varying Hamiltonian systems

MSC numbers. 34C37, 34C35, 34C23, 58F14, 34C20, 58F05, 34C29, 34C15

PAC numbers. 0545-a, 0230Hq, 4520Jj, 4510Hj

1. Introduction

Due to center manifold reduction, typical bifurcation theory (saddle-node, transcritical, and pitchfork) is one-dimensional (see [10], [11], and [12]). Even the amplitude for

Hopf bifurcation is one-dimensional. Lebovitz and Schaar analyzed one-dimensional transcritical [18] and pitchfork bifurcations [19] with the parameters slowly varying dynamically (in time). Haberman [13] showed how local first-order nonautonomous differential equations provided the transition between various slowly varying solutions and described circumstances under which a delayed bifurcation exists. Neishtadt [23], [24] proved that the unstable equilibrium may persist for slowly varying Hopf bifurcations. Haberman [13] also described slow bifurcations in conservative Hamiltonian systems, including pitchfork and transcritical, more recently studied by Mareé [20]. In the case of a saddle-center bifurcation, Haberman [13] showed how the first Painlevé transcendent provides a transition between small oscillations around the center and strongly nonlinear nearly homoclinic oscillations, which were then (1979) analyzed only in a preliminary fashion.

Slowly varying and weakly perturbed strongly nonlinear oscillations are analyzed by the method of averaging (see [1] and [26]), which has a long history. In particular it is known that action is an adiabatic invariant for Hamiltonian systems. The method of averaging is known to fail near an unperturbed homoclinic orbit (separatrix). For slowly varying Hamiltonian systems, Cary, Escande, and Tennyson [6] and Neishtadt [22] determined the $O(\epsilon \ln \epsilon)$ change in the action in the slow passage through a separatrix by considering a large sequence of nearly homoclinic orbits. Henrard [14] extensively analyzed the result of Cary, Escande, and Tennyson [6], and described many physical examples. Bourland and Haberman [2], [3], [4] analyzed the slow passage through a separatrix for systems with a small dissipative perturbation, obtaining an asymptotically accurate formula for the boundaries of the basins of attraction, generalizing Cary and Skodje [7]. Recently, Vainshtein, Vasiliev, and Neishtadt [25], [27] analyzed three-dimensional dynamical systems corresponding to stationary incompressible fluid flows with periodic solutions, calculating the small change in the adiabatic invariant due to the slow passage through a two-dimensional separatrix.

In this paper, the slow passage through a saddle-center bifurcation is studied. In Section 2 we review the method of averaging for strongly nonlinear oscillations that is valid away from the separatrix. In Section 3 we analyze nearly homoclinic orbits that are shown to be relevant before the saddle-center bifurcation has actually occurred, and in Section 4 we show how to use the averaged equations to obtain the boundary of the basin of repulsion. In Section 5, we analyze the strongly nonlinear saddle point and the corresponding saddle-center homoclinic orbit. The slow passage of a saddle-center homoclinic orbit is shown in Section 6 to consist of a large sequence of nearly saddle-center homoclinic orbits that are matched to the strongly nonlinear oscillations before and after passage. The sequence of times associated with the nonlinear saddle approaches are determined using the analytic continuation of the generalized Riemann zeta function (see the Appendix), which enables us to obtain in Section 7 the relatively large $O(\epsilon^{5/6})$ change in action in slowly crossing the saddle-center homoclinic orbit. In Section 8 we allow the energy to be particularly small at an approach to the saddle point so that the first Painlevé transcendent applies, in which case the solution usually either passes through the saddle-center bifurcation or approaches the center, but it is possible though unlikely that the solution approaches the saddle. An example is given in Section 9.

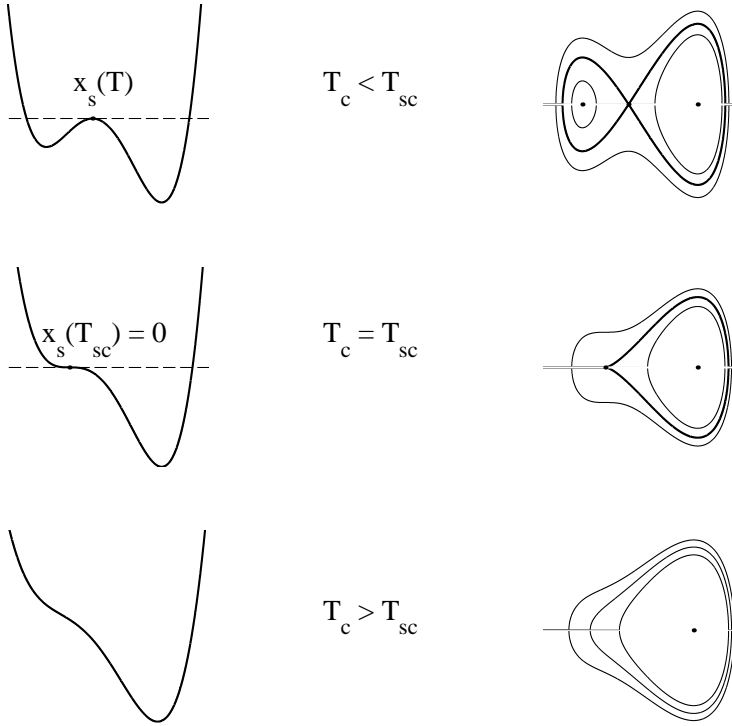


Fig. 1. Potential energy and phase portrait (fixed T) for saddle-center bifurcation.

2. Slowly Varying Strongly Nonlinear Oscillators

We analyze slowly varying conservative systems (a special case of slowly varying Hamiltonian systems)

$$\frac{d^2x}{dt^2} = f(x, T), \quad (2.1)$$

where $T = \epsilon t$ is the slow time scale and the slowly varying potential satisfies $V(x, T) = -\int_{x_s(T)}^x f(\bar{x}, T) d\bar{x}$. Slowly varying equilibria (saddles and centers) are characterized by $f(x_0(T), T) = 0$, which form the leading-order term in a unique asymptotic solution of (2.1). Here, we analyze a bounded saddle-center bifurcation so that we assume a saddle and center only exist for $T < T_{sc} = 0$ and coalesce there as is shown in Figure 1. In addition, we assume there is a second center which persists and, to be specific, stays to the right throughout the bifurcation. The corresponding bifurcation diagram corresponding to a saddle-center bifurcation is shown in Figure 2. It is important that the potential be defined relative to a slowly varying saddle point when there is a saddle ($T \leq T_{sc}$) so that $V_T(x_s, T) = 0$. At $T = T_{sc}$ there is a strongly nonlinear saddle point which we assume is located at $x = 0$. For $T > T_{sc}$ it is less important how the potential is measured so we assume it is zero at $x = 0$. The phase portraits with T fixed (see Fig. 1) have periodic and homoclinic orbits that only approximate solutions to (2.1).

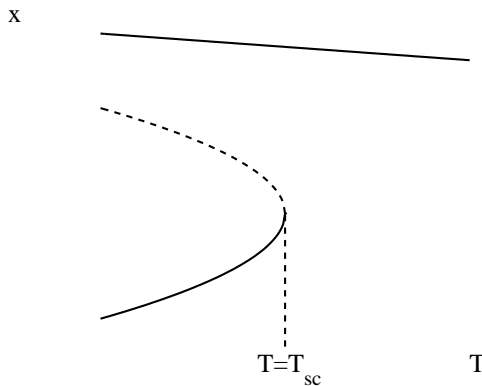


Fig. 2. Bifurcation diagram.

Away from the homoclinic orbits, solutions of (2.1) are slowly varying nonlinear oscillators. We use the method of averaging [1], [3], [26] with energy-angle coordinates

$$E = \frac{1}{2} \left(\frac{dx}{dt} \right)^2 + V(x, T), \quad (2.2)$$

$$\frac{\psi}{\omega(E, T)} = \int_{x_{min}}^x \frac{dx}{\sqrt{2[E - V(x, T)]^{1/2}}}, \quad (2.3)$$

where the x_{min} and x_{max} are the minimum and maximum of an oscillation and depend on E and T and where the frequency of a strongly nonlinear oscillator satisfies $\omega(E, T) = \{2 \int_{x_{min}}^{x_{max}} \frac{dx}{\sqrt{2[E - V(x, T)]^{1/2}}}\}^{-1}$. After a near identity transformation $E = e + \epsilon E_1(e, \phi, T) + \dots$ and $\psi = \phi + \epsilon \psi_1(e, \phi, T) + \dots$, where e and ϕ represent the average energy and phase, it can be shown that the leading-order averaged equations are particularly accurate and may be used (with care) in describing the slow passage through homoclinic orbits

$$\frac{de}{dT} = \omega(e, T)D(e, T) + O(\epsilon^2), \quad (2.4)$$

$$\frac{d\phi}{dt} = \omega(e, T) + O(\epsilon^2), \quad (2.5)$$

where $D(e, T) = \int_0^{1/\omega} V_T(x, T) dt$ is the change in energy over one period $\frac{1}{\omega}$. Action ($I = \int p dq$) is an adiabatic invariant ($\frac{dI}{dT} = 0$ since $I_e = \frac{1}{\omega}$ and $I_T = -D$), but we prefer to use the energy. These averaged equations represent three different kinds of nearly periodic solutions, those in the left (L) and right (R) wells and those solutions outside (Out) the wells. The method of averaging is known to fail near the unperturbed homoclinic orbits ($e = 0$).

3. Nearly Homoclinic Orbits ($T_c < T_{sc}$) for Slowly Varying Saddle-Center Bifurcation

Neishtadt [21] showed that it takes an intermediate time to cross the separatrix, a long time ($O(\ln \epsilon)$) in the fast time scale t but a short time ($O(\epsilon \ln \epsilon)$) in the slow time scale T . Specifically, the homoclinic orbit (separatrix) is crossed in a quasi-steady fashion with the slow time T nearly fixed at T_c , where T_c is the time at which the averaged equations (2.4) predict the averaged energy crosses the separatrix ($e = 0$). Near the unperturbed homoclinic orbit, the solution consists of a large sequence of nearly homoclinic orbits. The solution is approximated by a nearly homoclinic orbit between successive saddle approaches. The energy change ΔE from one saddle approach to the next is known to be accurately approximated by the corresponding homoclinic Melnikov (Poincaré-Arnold) integral $\epsilon \int_{-\infty}^{\infty} V_T(x, T_c) dt$, which depends on whether the solution x in the integrand is approximately a left or right homoclinic orbit, which in this slow variation case also depends on T_c

$$\Delta E = \begin{cases} \epsilon M_L(T_c), \\ \epsilon M_R(T_c). \end{cases} \quad (3.1)$$

The Melnikov change in energy is known to equal the change in energy for periodic solutions in the limit as the periodic solutions approach the homoclinic orbit, so that $D(0, T)$ equals $M_L(T)$, $M_R(T)$, or $M_L(T) + M_R(T)$, depending on whether the periodic solution is approximated by the left ($E < 0$), right ($E < 0$), or double homoclinic orbit ($E > 0$).

In order to investigate the simplest dynamics (forwards and backwards in time) of a saddle-center bifurcation, we will assume that each of the three Melnikov functions do not change signs and that the dissipation function for periodic solutions $D(E, T)$ also maintain the same signs as their corresponding Melnikov functions. There are two cases of interest corresponding to a saddle-center bifurcation:

$$I. \quad M_L(T_c) > 0, M_R(T_c) < 0, M_L(T_c) + M_R(T_c) < 0, \quad (3.2)$$

$$II. \quad M_L(T_c) > 0, M_R(T_c) > 0, M_L(T_c) + M_R(T_c) > 0. \quad (3.3)$$

We study case I in this paper because case II corresponds to the “usual” dissipation (backwards in time). The basic reason that $M_L(T_c) > 0$ is that solutions initially ($T = T_{initial} < T_{sc} = 0$) in the left well have $E < 0$ and must pass through the homoclinic orbit ($E = 0$) before the left well disappears ($T_c < T_{sc} = 0$). Thus, energy must increase for all of these solutions, and consequently $M_L(T_c) > 0$. A third case $M_L(T_c) > 0$, $M_R(T_c) < 0$, $M_L(T_c) + M_R(T_c) > 0$ cannot occur (assuming no sign changes) since the disappearance of the left well implies that $M_L(T_c) \rightarrow 0$ as $T_c \rightarrow T_{sc} = 0$. The following more explicit demonstration of $M_L(T_c) > 0$ may be of interest. The normal form (rescaled for simplicity) of the saddle-center bifurcation near $x = 0$, $T = T_{sc} = 0$ (with the left well disappearing) is $f \sim x^2 + T$, with saddle at $x \sim +\sqrt{-T}$ (since $f_x > 0$ there) and center at $x \sim -\sqrt{-T}$ (since $f_x < 0$ there). The corresponding potential (set to zero at the saddle point) is $V \sim -(\frac{x^3}{3} + Tx) - \frac{2}{3}(-T)^{3/2}$. Here $V_T \sim -x + (-T)^{1/2}$, and thus $V_T < 0$ for $x > (-T)^{1/2}$ and $V_T > 0$ for $x < (-T)^{1/2}$. This proves that $M_L(T) > 0$ for $T < T_{sc} = 0$ (and small) since the left region only involves x small,

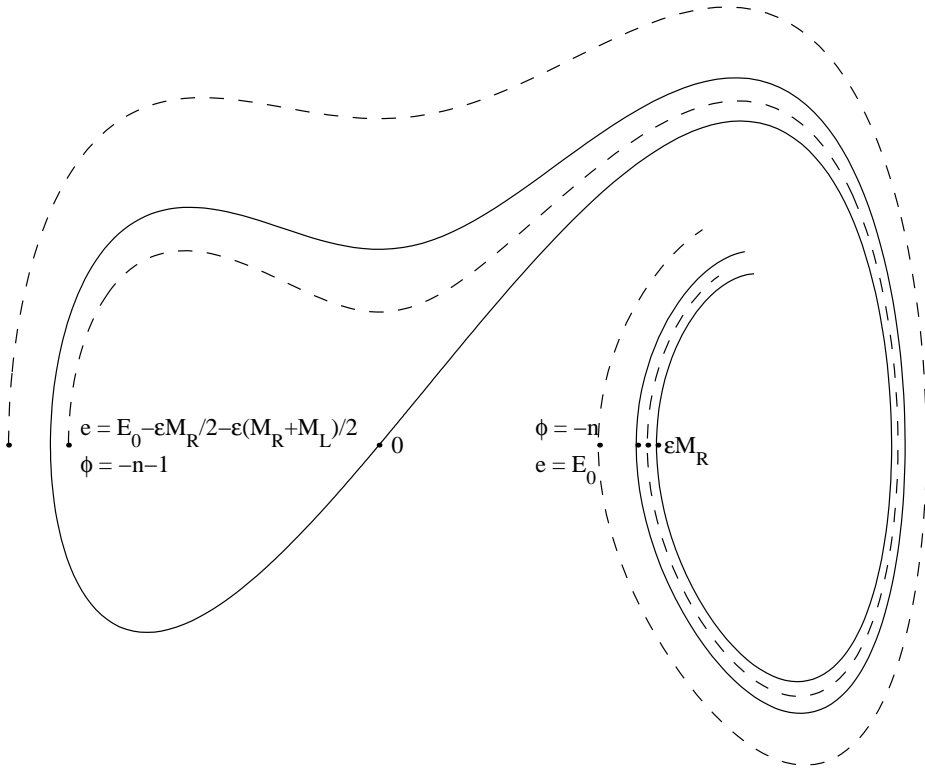


Fig. 3. Two branches of stable manifold (backwards in time) of saddle, boundaries of the basins of repulsion, exit saddle approach, and repelled orbits (dashed) from left and outer regions: $T_c < T_{sc}$ with $M_R(T_c) < 0$, $M_L(T_c) > 0$, $M_R(T_c) + M_L(T_c) < 0$.

but does not prove anything concerning $M_R(T)$ since the right well is not restricted to x small.

Orbits that correspond to the slow passage through the unperturbed homoclinic orbit for fixed $T = T_c$ (with $T_c < T_{sc} = 0$) are well-known and are shown in Figure 3. Since $M_L(T_c) > 0$, $M_R(T_c) < 0$, $M_L(T_c) + M_R(T_c) < 0$, all solutions are captured into the right well. Solutions that start in the left well (L) and those solutions that start in the top region (Out) outside the well form thin alternating bands. The energy at the exit saddle approach E_0 (last saddle approach with negative energy) ranges from $\epsilon M_R(T_c)$ to 0:

$$\epsilon M_R(T_c) < E_0 < 0. \quad (3.4)$$

The boundaries of the basins of repulsion are the two branches of the unstable manifolds of the saddle point, and their energies ($E_0 = \epsilon M_R(T_c)$ and $E_0 = \epsilon M_R(T_c) + \epsilon M_L(T_c)$ at the exit saddle approach can be computed using the Melnikov result (4.1). Thus, if

$$\epsilon M_R(T_c) < E_0 < \epsilon M_R(T_c) + \epsilon M_L(T_c), \quad (3.5)$$

then solutions originated in the left well (L), and if

$$\epsilon M_R(T_c) + \epsilon M_L(T_c) < E_0 < 0, \quad (3.6)$$

then solutions originated outside the wells (Out). The probabilities of release (opposite to capture) are discussed in Neishtadt [21]

$$P(Out) = \frac{M_R(T_c) + M_L(T_c)}{M_R(T_c)} \quad \text{and} \quad P(L) = \frac{-M_L(T_c)}{M_R(T_c)}. \quad (3.7)$$

These probabilities depend on the slow time T_c at which the slow variation equations predict the average energy is zero.

When solutions are near the unperturbed homoclinic orbit, there is a well-known large sequence of nearly homoclinic orbits, each surrounded by near saddle approaches with energy E_i . The change in energy from one saddle approach to another can be approximated by the appropriate Melnikov function. Solutions that go from the left to the right have the sequence LLLLLLRRRRRR, and the energy at the i th saddle approach satisfies

$$E_i = \begin{cases} E_0 + i\epsilon M_L(T_c), & i < 0, \\ E_0 + i\epsilon M_R(T_c), & i \geq 0. \end{cases} \quad (3.8)$$

Solutions which go from outside the double homoclinic orbit to the right have the sequence LRLRLRLRLRRRRRRRR, and the energy at the i th saddle approach is similar to (3.8) but account of the even and odd saddle approaches must be made.

4. Use of the Averaged Equations in Separatrix Crossing ($T_c < T_{sc}$)

In the slow crossing of a separatrix, energy terms of $O(\epsilon)$ are of particular importance. The method of averaging fails as the separatrix is approached. To overcome this, Neishtadt [22] and Cary, Escande, and Tennyson [6] used the method of matched asymptotic expansions to show that the sequence of nearly homoclinic orbits matches the method of averaging before and after the slow passage through a separatrix. The difference between the energy E and the average energy e is $O(\epsilon)$, and thus the $O(\epsilon)$ correction to the energy should be included. However, many authors including Bourland and Haberman [2] showed that this $O(\epsilon)$ energy difference vanishes at the minima and maxima of the orbits, and thus the averaged energy may be used directly at the minima and maxima.

Since all solutions that pass through the separatrix fall into the right well with negative energies, we consider final (instead of initial) conditions in the right well at $T = T_f$ with given energy $e(T_f) < 0$ and phase $0 \leq \phi(T_f) < 1$ far enough from the separatrix so that the averaging equations are valid there. The method of averaging (2.4) predicts that the average energy $e = 0$ at $T = T_c = \epsilon t_c$ where (2.5) predicts the phase to be ϕ_c . The separatrix is crossed with T fixed at T_c , and near the separatrix ($e = 0$) the averaged equations can be approximated by quasi-steady equations

$$\frac{de}{dT} \approx \omega(e, T_c) D(0, T_c), \quad (4.1)$$

$$\frac{d\phi}{dT} \approx \frac{\omega(e, T_c)}{\epsilon}, \quad (4.2)$$

where $D(0, T_c)$ is the relevant Melnikov integral evaluated at T_c predicted by the slow variation equations. Following Bourland and Haberman [3], [4], we note that near the separatrix, the average energy equation behaves as an autonomous equation, and thus the simple relationship follows:

$$\frac{de}{d\phi} = \epsilon D(0, T_c). \quad (4.3)$$

Consequently, for two different phases along an orbit using the averaged equations near the separatrix,

$$\Delta e = \epsilon D(0, T_c) \Delta \phi. \quad (4.4)$$

The two phases we use are $\phi = \phi_c$, where $e = 0$ and $\phi = -n < 0$ (it is important that this is an integer) where $e = E = E_0$. Since these calculations use averaging in the right well, $D(0, T_c) = M_R(T_c)$, and it follows from (4.4) that

$$E_0 = -\epsilon M_R(T_c)(n + \phi_c). \quad (4.5)$$

Using (3.5) and (3.6), we show that the number of orbits n equals the number predicted by slow variation theory, $n = \lceil -\phi_c \rceil$, the integral part of $-\phi_c$, and thus

$$E_0 = \epsilon M_R(T_c)(-\phi_c)^{mod} < 0, \quad (4.6)$$

where $(Q)^{mod}$ is the modulus or fractional part of Q . Furthermore, it follows from (4.6) using (3.5) and (3.6) that the specific repeller can be determined from initial conditions using slow variation theory. If

$$0 < (-\phi_c)^{mod} < \frac{M_R(T_c) + M_L(T_c)}{M_R(T_c)}, \quad (4.7)$$

then solutions originated outside the wells (Out), and if

$$\frac{M_R(T_c) + M_L(T_c)}{M_R(T_c)} < (-\phi_c)^{mod} < 1, \quad (4.8)$$

then solutions originated in the left well(L). The boundaries of the basins of repulsion (unstable manifolds of the saddle point) correspond to $(-\phi_c)^{mod} = 0$ and $(-\phi_c)^{mod} = \frac{M_R(T_c) + M_L(T_c)}{M_R(T_c)}$. In addition, this explains the probabilities (3.7). To obtain connection formulas for the averaged energy corresponding to slow passage (backwards in time) through the separatrix, we must also use slow variation theory for the nearly periodic solutions in the left wells and outside the wells.

For the left well, the slow variation theory will predict $e = 0$ at $T = T_L$ where $\phi = \phi_L$. We first determine ϕ_L in a straightforward manner (T_L is more difficult to determine, and we will describe this later). Again, Neishtadt [21] showed that T_L is near enough to T_c so that (4.1)–(4.5) again apply. In particular, we employ the averaged equation (4.4) with the following two phases along the orbit near the separatrix: $\phi = \phi_L$ where $e = 0$ and $\phi = -n - 1 < 0$ (again it is important that we choose this to be an integer) where $e = E = E_0 - \frac{\epsilon M_R(T_c)}{2} - \frac{\epsilon M_L(T_c) + \epsilon M_R(T_c)}{2}$ using the Melnikov idea for the

corresponding half orbits. Since these calculations are using averaging in the left well here $D(0, T_c) = M_L(T_c)$, and thus from (4.4),

$$-\phi_L = -\phi_c - \frac{1}{2} + \frac{M_R(T_c) - M_L(T_c)}{M_L(T_c)} [(-\phi_c)^{\text{mod}} - 1], \quad (4.9)$$

where (4.6) has been used. From (4.9) using (4.8), we can show that $[[-\phi_L]] = [[-\phi_c - \frac{1}{2}]]$ with no restrictions on $(-\phi_L)^{\text{mod}}$ as should be required. If the method of averaging were valid throughout, ϕ_L would equal ϕ_c , so that (4.9) shows that one effect of the slow passage (from the right well to the left well) through a homoclinic orbit is to introduce a phase jump:

$$\phi_{\text{jump}} = \frac{1}{2} - \frac{M_R(T_c) - M_L(T_c)}{M_L(T_c)} [(-\phi_c)^{\text{mod}} - 1]. \quad (4.10)$$

A similar calculation can be applied to orbits that finish outside the wells. The method of averaging predicts $e = 0$ at $T = T_{\text{out}}$ where $\phi = \phi_{\text{out}}$. As for the left well, T_{out} will be near enough to T_c for (4.1)–(4.5) to be valid with $D(0, T_c) = M_L(T_c) + M_R(T_c)$. Equation (4.4) is used along the orbit near the separatrix with $\phi = \phi_{\text{out}}$ where $e = 0$ and $\phi = -n - 1 < 0$ where, again $e = E = E_0 - \frac{\epsilon M_R(T_c)}{2} - \frac{\epsilon M_L(T_c) + \epsilon M_R(T_c)}{2}$. We obtain

$$-\phi_{\text{out}} = -\phi_c - \frac{M_L(T_c)}{M_L(T_c) + M_R(T_c)} \left[(-\phi_c)^{\text{mod}} - \frac{1}{2} \right], \quad (4.11)$$

where (4.6) has again been used. It follows from (4.11) using (4.7) that $[[-\phi_{\text{out}}]] = [[-\phi_c + \frac{\frac{1}{2} M_L(T_c)}{M_L(T_c) + M_R(T_c)}]]$ with again no restrictions on its modulus. If the method of averaging were valid throughout, ϕ_{out} would equal ϕ_c . Thus, from (4.11) one effect of passing slowly through a separatrix from the right well to oscillations outside the well is to introduce the phase jump:

$$\phi_{\text{jump}} = \frac{M_L(T_c)}{M_L(T_c) + M_R(T_c)} \left[(-\phi_c)^{\text{mod}} - \frac{1}{2} \right]. \quad (4.12)$$

The complete connection formulas also require the times T_L and T_{out} at which the averaged energy is predicted to be zero by slow variation theory after the slow passage through a homoclinic orbit. These times are comparatively difficult to calculate since they involve matching the sequence of saddle times. We omit this here since these times have been calculated in essentially equivalent situations by Cary, Escande, and Tennyson [6] and Bourland and Haberman [2], [4]. However, in Section 6 we will calculate these times by the same method for the related situation of the slow passage through a saddle-center homoclinic orbit.

In the preceding analysis, we have assumed that the predicted separatrix crossing time T_c is less than the saddle-center bifurcation time T_{sc} , in which case all the solutions cross the separatrix before the saddle-center bifurcation has occurred. If $T_c > T_{sc}$, then no separatrix crossing occurs, and the usual slow variation theory may be used without

modification (for example action is conserved). An interesting situation arises if $T_c = T_{sc}$ (we will also consider what happens if T_c is near T_{sc}).

5. Saddle-Center Homoclinic Orbit and a Strongly Nonlinear Saddle Point

At $T = T_{sc}$, there is a one-branched homoclinic orbit connecting the strongly nonlinear saddle point at $x = 0$ (where the energy is zero) to itself (see Fig. 1). The potential can be approximated by a cubic at $T = T_{sc}$,

$$V(x, T_{sc}) \approx -\beta x^3, \quad (5.1)$$

with $6\beta = -V_{xxx}(0, T_{sc}) = f_{xx}(0, T_{sc}) > 0$. The time-dependence of the “saddle-center” homoclinic orbit is described by

$$\int_{x_{max}}^x \frac{d\bar{x}}{\sqrt{2}\sqrt{-V(\bar{x}, T_{sc})}} = -|t - t_i^*|, \quad (5.2)$$

where t_i^* is the center (symmetry) time of this solitary pulse at which $x = x_{max}$ when $T = T_{sc}$. This solitary pulse corresponds to the energy being a constant $E = 0$. However, solutions take a long time to slowly pass through this kind of separatrix (as with the one characterized by a linear saddle point). Thus, the solution will be approximated by a large sequence of nearly solitary pulses of this kind which we parameterize by the symmetry time t_i^* . Although the energy is slowly varying, this homoclinic orbit will be sufficiently accurate for our purposes, since higher order terms away from the saddle point will be accounted for using the Melnikov integral for the change in the energy due to a slowly varying potential. When the effect of the slow variation is included, the homoclinic orbit is broken, and orbits spiral inwards as we have assumed $M_R(T_c) < 0$ as also indicated in Figure 4.

To obtain the asymptotic expansion of this saddle-center homoclinic orbit as $t - t_i^* \rightarrow \pm\infty$, we add and subtract the singularity using (5.1) and obtain

$$x \sim \frac{2}{\beta(|t - t_i^*| - c)^2}, \quad \text{as } t - t_i^* \rightarrow \pm\infty, \quad (5.3)$$

where $c = -\sqrt{\frac{2}{\beta x_{max}}} + \int_0^{x_{max}} [\frac{1}{\sqrt{2}\sqrt{-V(x, T_{sc})}} - \frac{1}{\sqrt{2\beta x^3}}] dx$. Note that the solitary pulse associated with the saddle-center bifurcation decays algebraically toward the strongly nonlinear saddle point, unlike the usual solitary pulses associated with linear saddle points which decay exponentially.

Solutions pass near the strongly nonlinear saddle point many times, which we characterize by the energy E_i and the time of closest approach t_i . We will define these more precisely. In the neighborhood of the strongly nonlinear saddle ($x = 0$), the leading-order differential equation is a sufficiently accurate approximation for our purposes,

$$\frac{d^2x}{dt^2} = 3\beta x^2, \quad (5.4)$$

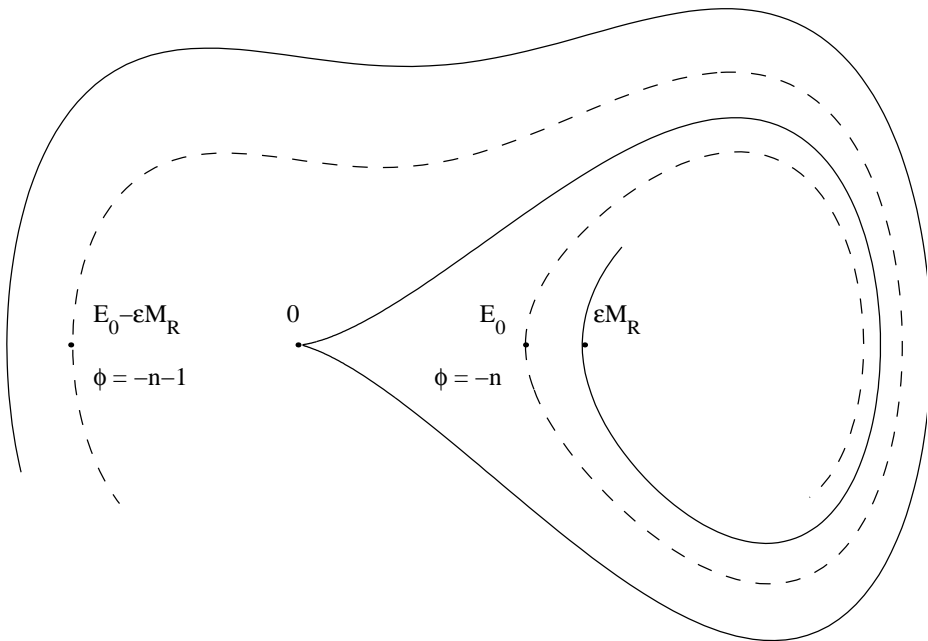


Fig. 4. Stable and unstable manifolds of saddle at saddle-center bifurcation: $T_c = T_{sc}$ with $M_R(T_{sc}) < 0$. The exit region is defined by $\epsilon M_R(T_{sc}) < E_0 < 0$.

which satisfies conservation of energy

$$\frac{1}{2} \left(\frac{dx}{dt} \right)^2 - \beta x^3 = E_i, \tag{5.5}$$

with phase portrait as shown in Figure 5. $E_i = 0$ corresponds to exactly a stable or unstable manifold of the nonlinear saddle point, and (5.5) yields the simple result $x =$

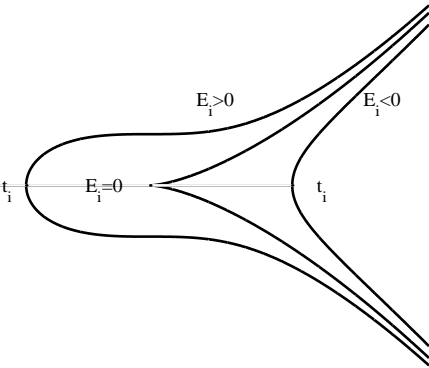


Fig. 5. Nonlinear saddle point at saddle-center bifurcation.

$\frac{2}{\beta(t-k)^2}$. Of greater interest to us will be $E_i \neq 0$, in which case it is best to rescale (5.5) (especially since we will later make assumptions concerning the size of E_i)

$$x = \left| \frac{E_i}{\beta} \right|^{1/3} \bar{x}, \quad (5.6)$$

$$t - t_i = |E_i \beta^2|^{-1/6} \bar{t}, \quad (5.7)$$

where $t = t_i$ ($\bar{t} = 0$) corresponds to the “nearest” saddle approach (minimum where $\frac{dx}{dt} = 0$) or symmetry time for (5.5). This scaling shows that there are two versions of (5.5) depending on whether the energy at the nonlinear saddle approach is negative or positive:

$$\frac{1}{2} \left(\frac{d\bar{x}}{d\bar{t}} \right)^2 - \bar{x}^3 = \pm 1, \quad (5.8)$$

where the upper sign in (5.8) corresponds to $E_i > 0$ and vice versa. We use this same sign convention for many subsequent equations. The solution of (5.8) is

$$\frac{1}{\sqrt{2}} \int_{\mp 1}^{\bar{x}} \frac{dx}{(x^3 \pm 1)^{1/2}} = |\bar{t}|. \quad (5.9)$$

Solutions of (5.5) develop a finite time singularity ($\bar{x} \rightarrow +\infty$) according to (5.9) at

$$t_{\pm} = \frac{1}{\sqrt{2}} \int_{\mp 1}^{\infty} \frac{dx}{(x^3 \pm 1)^{1/2}} = \frac{\Gamma(\frac{1}{3})\Gamma(\frac{1}{6})}{2\sqrt{6}\pi} \bullet \begin{cases} 1, & E_i < 0, \\ \sqrt{3}, & E_i > 0, \end{cases} \quad (5.10)$$

forwards and backwards in time at $\bar{t} = t_{\pm}$ and at $\bar{t} = -t_{\pm}$. The asymptotic expansion of the singularity associated with the strongly nonlinear saddle point may be analyzed from (5.9) but it is perhaps simpler to obtain the result directly from the differential equation (5.4) or (5.5) once the singularity time is known (see (5.7) and (5.10)):

$$x \sim \frac{2}{\beta(t - t_{sing})^2} - \frac{\beta E_i}{28} (t - t_{sing})^4 + \dots \quad (5.11)$$

Note that this double-pole singularity at $t = t_{sing}$, where $|t_{sing} - t_i| = |E_i \beta^2|^{-1/6} t_{\pm}$, will match to the algebraic decay (5.3) of the solitary pulse. By including the small but necessary $O(t - t_{sing})^4$ term at the singularity, the differential equation is able to communicate the value of the energy as we will describe.

We use a notation (see Fig. 6) where the saddle-center homoclinic orbit centered at $t = t_i^*$ is preceded by the i th strongly nonlinear saddle approach t_i and followed by the $i + 1$ st strongly nonlinear saddle approach t_{i+1} . By matching this solitary pulse to the both strongly nonlinear saddles, we have to leading-order

$$t_i^* - t_i = |E_i \beta^2|^{-1/6} t_{\pm} + c, \quad (5.12)$$

$$t_{i+1} - t_i^* = |E_{i+1} \beta^2|^{-1/6} t_{\pm} + c. \quad (5.13)$$

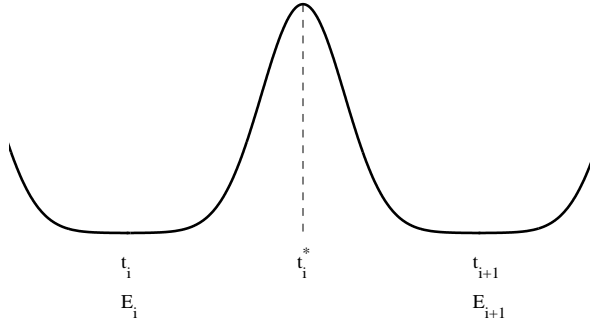


Fig. 6. Consecutive saddle-points surrounding a nearly saddle-center homoclinic orbit.

By adding (5.12) and (5.13), we obtain a difference equation for successive saddle times

$$t_{i+1} - t_i = |E_i \beta^2|^{-1/6} t_{\pm} + |E_{i+1} \beta^2|^{-1/6} t_{\pm} + 2c. \quad (5.14)$$

If the energy were constant, then $t_{i+1} - t_i$ represents the energy-dependent period. Thus, the asymptotic expansion of the period $P(E)$ of the periodic solution near the infinite period homoclinic orbit for small E is

$$\frac{1}{\omega(E)} = P(E) \sim 2 |E \beta^2|^{-1/6} t_{\pm} + 2c, \quad (5.15)$$

so that (5.14) represents the average of the two periods associated with a periodic solution of energies E_i and E_{i+1} . Here the energy is not constant, but can be determined by the Melnikov energy for the right homoclinic orbit (in the limit as the saddle-node bifurcation is approached):

$$E_{i+1} - E_i = \epsilon M_R(T_{sc}). \quad (5.16)$$

The exit region (see Fig. 4) $\epsilon M_R(T_{sc}) < E_0 < 0$ is defined by the unique unstable manifold of the strongly nonlinear saddle (the unique stable branch is less important). The sequence of energies is simple but important,

$$E_i = E_0 + \epsilon M_R(T_{sc})i, \quad (5.17)$$

which is valid for positive and negative integers i . The solution consists of a sequence of nearly saddle-center homoclinic orbits satisfying (5.17) which matches to the outside orbits (backwards in time) and the right orbits (forwards in time).

From (5.11), this change in energy (5.16) corresponds to the change in the $O((t - t_{sing})^4)$ term of the asymptotic expansion of the strongly nonlinear saddle. To find the change in energy without using the Melnikov result (5.16), one calculates the $O(\epsilon)$ perturbation to the solitary saddle-center homoclinic orbit and matches the resulting outer solution to the leading-order solution in the neighborhood of the nonlinear saddle. The $O(\epsilon)$ outer solution must contribute a term $\epsilon A_{\pm}(|t - t_i^*| - c)^4$. Thus, $-\frac{\beta E_i}{28} = \epsilon A_-$ and $-\frac{\beta E_{i+1}}{28} = \epsilon A_+$, so that

$$E_{i+1} - E_i = \epsilon M_R(T_{sc}) = -\epsilon \frac{28}{\beta} \text{ change in the } O((t - t_{sing})^4) \text{ coefficient.} \quad (5.18)$$

6. Slow Crossing of a Saddle-Center Homoclinic Orbit

Since the Melnikov function that accurately approximates the change in energy is the same before and after the exit saddle approach, we show the method of averaging may be used directly to minimums and maximums without a jump in phase. The method of averaging (2.4) predicts the average energy $e = 0$ at $T = T_c$ where (2.5) is used to calculate the corresponding average phase $\phi = \phi_c$, and for the passage to involve the saddle-center homoclinic orbit the condition again is that $T_c = T_{sc} = 0$. The sequence of strongly nonlinear saddle approaches (5.16) are valid. We again use (4.3) for the averaged energy $e(T)$, here with $D(0, T_c) = M_R(T_{sc})$ so that (4.4) becomes $\Delta e = \epsilon M_R(T_{sc}) \Delta \phi$ both before and after passage through the saddle-center homoclinic orbit. After passage we choose $e = 0$ where $\phi = \phi_c < 0$ and $e = E_0$ where $\phi = -n$, so that $n = \lceil -\phi_c \rceil$ and (4.6) follows:

$$E_0 = \epsilon M_R(T_{sc})(-\phi_c)^{mod} < 0, \quad (6.1)$$

so that we can determine E_0 from final (or initial) conditions. Before passage, we choose $e = 0$ at the unknown $T = T_{out}$ where $\phi = \phi_{out}$ and $e = E_0 - \epsilon M_R(T_{sc})$ where $\phi = -n - 1$, and we immediately obtain

$$\phi_{out} = \phi_c, \quad (6.2)$$

so that the method of multiple scales does not need to be modified in passing through a saddle-center homoclinic orbit. In slowly crossing the saddle-center homoclinic orbit, the solution obtained by the method of averaging is valid at minimums and maximums near the unperturbed homoclinic orbit, though a more accurate description consists of the large sequence of nearly homoclinic orbits described by (5.14) and (5.16). These should be matched using the method of matched asymptotic expansions because we will show the time predicted by the method of averaging is incorrect.

The sequence of approximately saddle-center homoclinic orbits is matched forwards and backwards in time to the solution obtained by averaging. Earlier, we have matched the energies. Here we match the saddle times. The times t_i of the saddle approaches associated with $T_c = T_{sc}$ satisfy (5.14), which is a difference equation for the successive saddle times

$$\begin{aligned} t_{i+1} - t_i &= |E_0 + \epsilon M_R(T_{sc})i|^{-1/6} \frac{t_{\pm}}{\beta^{1/3}} \\ &+ |E_0 + \epsilon M_R(T_{sc})(i+1)|^{-1/6} \frac{t_{\pm}}{\beta^{1/3}} + 2c, \end{aligned} \quad (6.3)$$

after using (5.17). We obtain from (6.3) the asymptotic expansion (top sign corresponds to $E > 0$ and vice versa) as $i \rightarrow \mp\infty$

$$t_i \sim \mp 2 |\epsilon M_R(T_{sc})|^{-1/6} \frac{6}{5\beta^{1/3}} |i|^{5/6} t_{\pm} + 2ci + \gamma_{\pm}, \quad (6.4)$$

where the size $O(\epsilon^{-1/6})$ of the constants γ_{\pm} are important. These constants cannot be determined from the form of the asymptotic expansion, but we will determine these constants using an explicit solution of (6.3) involving t_0 and the generalized Riemann

zeta function. The time-dependent averaged equations $\frac{de}{dT} = \omega(e, T)D(e, T)$ may be approximated near the unperturbed saddle-center homoclinic orbit by $(2|e\beta^2|^{-1/6}t_{\pm} + 2c)\frac{de}{dT} = M_R(T_{sc})$ using (5.15). Thus, at the saddle approaches,

$$\pm 2\frac{6}{5\beta^{1/3}}|E_i|^{5/6}t_{\pm} + 2cE_i = \begin{cases} M_R(T_{sc})(T_i - T_{out}), & E_i > 0, \\ M_R(T_{sc})(T_i - T_c), & E_i < 0, \end{cases} \quad (6.5)$$

where we have replaced e by E_i since the saddle approaches for the saddle-center homoclinic orbit are minimums of the orbit. (Equation (6.5) explicitly shows the averaged equations predict $e = 0$ in a finite time.) When (5.17) is substituted into (6.5), we see that the saddle times given by (6.4) are compatible only if

$$T_c = T_{sc} = \epsilon\gamma_- - \frac{2cE_0}{M_R} \quad \text{and} \quad T_{out} = \epsilon\gamma_+ - \frac{2cE_0}{M_R}. \quad (6.6)$$

The jump in fast time is large

$$t_{out} - t_c = \gamma_+ - \gamma_-, \quad (6.7)$$

so that the method of averaging makes large errors in time since $\gamma = O(\epsilon^{-1/6})$, but the jump in slow time is small, confirming that the passage of a saddle-center homoclinic orbit is done in a quasi-steady fashion.

The constants in (6.4), the asymptotic expansion as $i \rightarrow \mp\infty$ of the saddle times satisfying the difference equation (6.3), are obtained relatively easily from $\sum_{n=0}^{i-1} (a+n)^{-1/6} \sim \frac{6}{5}i^{5/6} + \zeta(\frac{1}{6}, a)$, which is derived in the appendix using the analytic continuation of the generalized Riemann zeta function, $\zeta(\frac{1}{6}, a)$:

$$\gamma_{\pm} = t_0 + |\epsilon M_R(T_{sc})\beta^2|^{-1/6}, \begin{cases} -2t_+\zeta\left(\frac{1}{6}, 1 - \frac{E_0}{\epsilon M_R}\right) - t_-\left(\frac{E_0}{\epsilon M_R}\right)^{-1/6}, \\ t_-\left[2\zeta\left(\frac{1}{6}, \frac{E_0}{\epsilon M_R}\right) - \left(\frac{E_0}{\epsilon M_R}\right)^{-1/6}\right]. \end{cases} \quad (6.8)$$

We recall that the energies $E_i > 0$ (corresponding to the first of (6.8)) for $i < 0$ and $E_i < 0$ for $i \geq 0$ (corresponding to the second of (6.8)). To derive (6.8), we have utilized some elementary ideas such as $(i+1)^{5/6} \sim i^{5/6}$, shifting sums, and letting $j = -i$ for $i < 0$. From (6.8), we have an explicit expression for the jump in the fast time

$$\begin{aligned} t_{out} - t_c &= \gamma_+ - \gamma_- \\ &= -2|\epsilon M_R(T_{sc})\beta^2|^{-1/6} \left[t_-\zeta\left(\frac{1}{6}, \frac{E_0}{\epsilon M_R}\right) + t_+\zeta\left(\frac{1}{6}, 1 - \frac{E_0}{\epsilon M_R}\right) \right], \end{aligned} \quad (6.9)$$

where from (6.1),

$$0 < \frac{E_0}{\epsilon M_R(T_{sc})} = (-\phi_c)^{mod} < 1. \quad (6.10)$$

In Section 8, we show (6.9) is not valid near the boundaries where $E_0 = O(\epsilon^{6/5})$ or $E_0 - \epsilon M_R(T_{sc}) = O(\epsilon^{6/5})$.

7. Change in Action for Slow Passage of a Saddle-Center Homoclinic Orbit

Action $I(e(T), T)$ is an adiabatic invariant before and after the slow passage through a saddle-center homoclinic orbit. Following Bourland and Haberman [4], the two different constants can be expressed as $I(e(T), T) = I(0, T_c)$ and $I(e(T), T) = I(0, T_{out})$. Since $T_c = T_{sc} \neq T_{out}$, but $T_{out} - T_c = O(\epsilon^{5/6})$, the jump in action when slowly crossing a saddle-center bifurcation is $O(\epsilon^{5/6})$ and is given by

$$\Delta I = I(0, T_{out}) - I(0, T_c) \sim I_T(0, T_{sc})(T_{out} - T_c) = -M_R(T_{sc})(T_{out} - T_c). \quad (7.1)$$

Using (6.9), we obtain

$$\Delta I = -\frac{2}{\beta^{1/3}} \epsilon^{5/6} |M_R(T_{sc})|^{5/6} \left[t_- \zeta \left(\frac{1}{6}, \frac{E_0}{\epsilon M_R} \right) + t_+ \zeta \left(\frac{1}{6}, 1 - \frac{E_0}{\epsilon M_R} \right) \right], \quad (7.2)$$

where $\zeta(\frac{1}{6}, a)$ is the analytic continuation of the generalized Riemann zeta function and where we note (6.10). This change in action is slightly larger than the $O(\epsilon \ln \epsilon)$ change in action derived by Neishtadt [22] and Cary, Escande, and Tennyson [6] for the slow passage through double-homoclinic orbits (with linear saddle points).

8. Nonautonomous Saddle-Point (the First Painlevé Transcendent) and the Transitions to the Center and Saddle

For slowly varying conservative or Hamiltonian systems, the earlier parts of this paper show that saddle-center bifurcations usually involve the connection of two strongly nonlinear oscillations by a large sequence of nearly homoclinic orbits. There is another family of somewhat different solutions in which there is a transition between strongly nonlinear oscillations near the saddle-center homoclinic orbit and solutions near the center or saddle involved in the saddle-center bifurcation.

We have described the leading-order nonlinear saddle point by the autonomous differential equation (5.4) with $\frac{1}{2}f_{xx} = 3\beta$. However, a more accurate approximation to the differential equation (2.1) near the nonlinear saddle point $x = 0$ at $T = T_{sc}$ would be the nonautonomous equation (Ince [15]) known as the first Painlevé transcendent,

$$\frac{d^2x}{dt^2} = \frac{1}{2}f_{xx}x^2 + f_T(T - T_{sc}), \quad (8.1)$$

where $T = \epsilon t$. Haberman [13] used the first Painlevé transcendent to describe this kind of transitional though he did not understand the details of the slow passage through a separatrix at that time (1979). (If T is near T_{sc} the unfolding would yield an equivalent equation $\frac{d^2x}{dt^2} = \frac{1}{2}f_{xx}x^2 + \lambda x + f_T(T - T_{sc})$ since it can be converted to (8.1) by shifting x and T .) If $T - T_{sc} \ll x^2$ near the strongly nonlinear saddle, then the previous analysis in the present paper for a saddle-center bifurcation is valid. Because the change of energy due to Melnikov ideas is $O(\epsilon)$, we may assume in our earlier analysis that the energy E_i itself is $O(\epsilon)$. From (5.5)–(5.7), this implies that $x = O(\epsilon^{1/3})$ and $t - t_{sc} = O(\epsilon^{-1/6})$, in which case $T - T_{sc} \ll x^2$ since $\epsilon^{5/6} \ll \epsilon^{4/6}$. Thus, the strongly nonlinear saddle is the

leading-order equation almost all the time. However, if x is even smaller (closer to the saddle), then it is possible for the first Painlevé (8.1) to be valid. The first Painlevé (8.1) involves the balance of the three terms only if

$$x = O(\epsilon^{2/5}) \quad \text{and} \quad t - t_{sc} = O(\epsilon^{-1/5}). \quad (8.2)$$

Here x is smaller than the scaling associated with the nonlinear saddle point ($\epsilon^{2/5} \ll \epsilon^{1/3}$). The first Painlevé with scaling (8.2) still occurs at an intermediate time scale (slow from the point of view of the fast time t , but fast from the point of view of the slow time T) since $T - T_{sc} = O(\epsilon^{4/5})$. The corresponding energy E_i defined by (5.5) is $O(\epsilon^{6/5})$, much less than the $O(\epsilon)$ energy associated with our previous sequence of nonlinear saddle approaches. Since our sequence of saddle approaches will remain valid (backward in time), this can only occur if one of the sequence of saddle approaches is near the boundary of the basin of repulsion, i.e., either

$$E_0 = O(\epsilon^{6/5}) \quad \text{or} \quad E_0 - \epsilon M_R(T_{sc}) = O(\epsilon^{6/5}). \quad (8.3)$$

Philosophically, this can arise differently forward or backward in time. Forward in time, as we will show, requires the transition to be near the coalescing saddle-center, while backward in time puts constraints on the “final” energy such that the energy is almost precisely zero at a saddle approach as described by (8.3).

In analyzing the passage through various kinds of bifurcations, Haberman [13] showed that there are slowly varying solutions of (1.1), $x_{sv} \sim x_0(T) + \epsilon^2 \frac{x_{0T}}{f_x} + \dots$, whose leading-order behavior satisfies $0 = f(x_0, T)$. To analyze solutions near a slowly varying bifurcating center, we summarize Haberman [13] who used the method of multiple scales with a slow time T and the usual fast phase associated with linear Liouville-Green type asymptotics. When weakly nonlinear effects were included, the following solution was obtained near the slowly varying center but away from the bifurcation point:

$$x \sim x_{sv}(T) + 2A\epsilon^{1/2}k^{-1/4} \cos \left[\frac{\int_0^T k^{1/2} d\bar{T}}{\epsilon} + \phi_1(T) \right], \quad (8.4)$$

where $k = -f_x(x_{sv}) = V_{xx}(x_{sv})$ and $k^{1/2}$ is nearly the linear circular frequency. The phase shift $\phi_1(T)$ was shown to satisfy $\frac{d}{dT}\phi_1(T) = -\frac{A^2}{12k}(3f_{xxx} + \frac{2}{k}f_{xx}^2)$. At the saddle-center bifurcation $f_x(0, T_{sc}) = 0$, so that $f \sim \frac{1}{2}f_{xx}x^2 + f_T(T - T_{sc})$, where from now on these derivatives are evaluated at $(0, T_{sc})$, in which case $f_{xx} = 6\beta$; see (5.1). The center of the center-saddle bifurcation satisfies $x_0 \sim -(\frac{2f_T}{f_{xx}})^{1/2}(T_{sc} - T)^{1/2}$ so that $k \sim -f_{xx}x_0$ as the saddle-center bifurcation is approached. In the case of the slowly varying center of the saddle-center bifurcation (at $x = 0$ at $T = T_{sc}$) as $T \rightarrow T_{sc}$,

$$\begin{aligned} x \sim & -\left(\frac{f_T}{3\beta}\right)^{1/2} (T_{sc} - T)^{1/2} + \dots \\ & + \epsilon^{1/2} \frac{2A \cos[-(12\beta f_T)^{1/4} \frac{4(T_{sc}-T)^{5/4}}{5\epsilon} + \frac{A^2\beta}{2f_T} \ln(T_{sc} - T) + \theta]}{[12\beta f_T(T_{sc} - T)]^{1/8}}. \end{aligned} \quad (8.5)$$

(The stable manifold of the slowly varying saddle point can be obtained in a similar way.) This outer expansion (8.5) fails when $T_{sc} - T = O(\epsilon^{4/5})$ with $x = O(\epsilon^{2/5})$ giving

rise to the scalings (8.2) of the first Painlevé. In particular we introduce the scaling of the special nonautonomous nonlinear saddle point

$$x = \epsilon^{2/5} \frac{f_T^{2/5}}{(3\beta)^{3/5}} w, \quad (8.6)$$

$$T - T_{sc} = \epsilon^{4/5} \frac{1}{(3\beta f_T)^{1/5}} \tau, \quad (8.7)$$

so that the normalized first Painlevé arises

$$\frac{d^2 w}{d\tau^2} = w^2 + \tau. \quad (8.8)$$

The asymptotic expansions of the first Painlevé are well known [15]. Using a Boutroux transformation, the asymptotic expansion backwards in time of the first Painlevé usually either explodes or approaches the stable center, qualitatively similar to the phase portrait of the left well in Figure 3. These solutions are separated by the stable manifold (backwards in time) of the saddle point. Solutions may oscillate around the center, approaching the center backwards in time

$$w \sim -(-\tau)^{1/2} + A_p(-\tau)^{-1/8} \cos \left[\frac{4\sqrt{2}}{5}(-\tau)^{5/4} - \frac{A_p^2 \sqrt{2}}{24} \ln(-\tau) + \theta_p \right], \quad (8.9)$$

as $\tau \rightarrow -\infty$. This clearly matches to the oscillations around the slowly varying center given by (8.5). All solutions of the first Painlevé develop a finite time singularity as $\tau \rightarrow \tau_p$ forwards in time:

$$w \sim 6(\tau - \tau_p)^{-2} - \frac{\tau_p}{10}(\tau - \tau_p)^2 - \frac{1}{6}(\tau - \tau_p)^3 + c_p(\tau - \tau_p)^4 + \dots \quad (8.10)$$

A solution of (8.8) can also have finite time singularities forward and backwards in time. The solutions of the first Painlevé provide connections so that (A_p, θ_p) should be determined by the two parameters associated with the singularity (τ_p, c_p) and vice versa. Explicit connection formulas now exist by isomonodromy methods [9], [16], [17]. The asymptotic expansion of the singularity of the first Painlevé can be seen to be slightly different than the singularity of the autonomous nonlinear saddle point (5.11).

Haberman [13] showed that the finite time singularity of the first Painlevé matches into a nearly solitary pulse associated with the saddle-center bifurcation that is followed by a sequence of such nearly homoclinic orbits. The singularity of the first Painlevé matches to the algebraic decay (5.3) of the first saddle-center homoclinic orbit centered at $t = t_0^*$ (which we will determine in this way):

$$t_0^* - t_{sc} = (3\beta \epsilon f_T)^{-1/5} \tau_p + c. \quad (8.11)$$

It is most important that the order of magnitude of the time shift is $O(\epsilon^{-1/5})$ again an intermediate time scale, this one associated with the nonautonomous nonlinear saddle point. The shift of the center time is longer than the $O(\epsilon^{-1/6})$ time associated with the

“usual” strongly nonlinear saddle point since the solution passes even closer to the saddle point.

We may think of the coefficient of $(t - t_{sing})^4$ as equaling $-\frac{\beta E_0}{28}$. Using (8.10) with (8.6) and (8.7), we obtain

$$E_0 = -\frac{28}{\beta}(\epsilon f_T)^{6/5}(3\beta)^{1/5}c_p. \quad (8.12)$$

It is important that the energy is small $O(\epsilon^{6/5})$ where the first Painlevé is valid. The energy is determined from the important coefficient c_p of the $(\tau - \tau_p)^4$ term in the singularity (8.10) of the first Painlevé. The energy is not constant at a saddle approach described by the first Painlevé so that (8.12) only describes the correct coefficient of the fourth power necessary to predict the energy at the next saddle approach,

$$E_1 = -\frac{28}{\beta}(\epsilon f_T)^{6/5}(3\beta)^{1/5}c_p + \epsilon M_R(T_{sc}), \quad (8.13)$$

which will not be approximately zero. Thus, this and all subsequent saddle points will be described by the usual nonlinear saddle for saddle-center bifurcation (not the first Painlevé). In between these saddle approaches, the solution will be the nearly saddle-center homoclinic orbit, so that the energies at the subsequent saddle approaches are determined using Melnikov ideas,

$$E_i = -\frac{28}{\beta}(\epsilon f_T)^{6/5}(3\beta)^{1/5}c_p + \epsilon M_R(T_{sc})i. \quad (8.14)$$

The times of the saddle approaches may be obtained as we did earlier from a sequence of nearly saddle-center homoclinic orbits so that (5.14) may be used:

$$t_{i+1} - t_i = |E_i \beta^2|^{-1/6} t_{\pm} + |E_{i+1} \beta^2|^{-1/6} t_{\pm} + 2c. \quad (8.15)$$

Equation (8.14) is used for the energy.

These solutions near the saddle-center homoclinic orbit will match (as before) to strongly nonlinear oscillations obtained by the method of averaging. We can use our previously derived energy result, (6.1), with E_0 given by (8.12):

$$E_0 = -\frac{28}{\beta}(\epsilon f_T)^{6/5}(3\beta)^{1/5}c_p = \epsilon M_R(T_{sc})(-\phi_c)^{mod} < 0. \quad (8.16)$$

There is a thin band of solutions with $(-\phi_c)^{mod} = O(\epsilon^{1/5})$ corresponding to the first Painlevé if $c_p \geq 0$. If $c_p < 0$, then $E_0 > 0$, which means that E_1 is close to $-\epsilon M_R(T_{sc})$ as allowed (and E_1 , not E_0 , corresponds to the first Painlevé). Equation (8.16) can be used forward in time, giving matching conditions that the strongly nonlinear oscillation must satisfy. It is perhaps more natural to interpret (8.16) backwards in time. We can obtain the first Painlevé only for very special final conditions from which the energy is predicted to be even smaller than usual; the energy needs to be $O(\epsilon^{6/5})$ rather than $O(\epsilon)$.

The saddle approach times t_i are used to determine the singularity time τ_p from final conditions. The sequence of saddle times satisfies (8.15) and starts from t_1 . However, the

energy is much closer to zero (and the resulting period much larger) only for the saddle point that satisfies the first Painlevé. Thus, in computing the saddle approach times, it will be a valid approximation to replace E_0 by 0 everywhere except $i = 0$. In this case, (8.15) simplifies and its asymptotic expansion is determined using (A.6). We compare the asymptotic expansion to (6.4) and obtain

$$\gamma_- = t_1 - 2c + 2 |\epsilon M_R(T_{sc}) \beta^2|^{-1/6} t_- \left[\zeta \left(\frac{1}{6}, 1 \right) - \frac{1}{2} \right]. \quad (8.17)$$

It should be noted that $\zeta(\frac{1}{6}, 1) = \zeta(\frac{1}{6})$ is the usual Riemann zeta function. γ_- is determined from final conditions (6.6), so that (8.17) shows how t_1 is determined from final conditions. Knowing t_1 gives t_0^* from (5.13), so that τ_p is determined from (8.11) using (5.13):

$$(3\beta\epsilon f_T)^{-1/5} \tau_p + 2 |\epsilon M_R(T_{sc}) \beta^2|^{-1/6} t_- \zeta \left(\frac{1}{6}, 1 \right) = t_c - t_{sc}. \quad (8.18)$$

Note that $t_c - t_{sc}$ is large while $\epsilon(t_c - t_{sc}) = T_c - T_{sc}$ is small. We would be justified in keeping the smaller $O(\epsilon^{-1/6})$ term in (8.18) only if (5.13) and (8.17) are accurate to $o(\epsilon^{-1/5})$.

As in Section 7, action is an adiabatic invariant before and after the slow passage through the saddle-center bifurcation. When the solution, (8.4) and (8.9), is a linear oscillation around the slowly varying equilibrium, the action is well-known to be approximated by $4\pi\epsilon A^2 = \frac{\pi\sqrt{2}f_T}{3\beta}\epsilon A_p^2$. Thus, the change in action is

$$\begin{aligned} \Delta I &= 4\pi\epsilon A^2 - I(0, T_c) \sim 4\pi\epsilon A^2 - I(0, T_{sc}) - I_T(0, T_{sc})(T_c - T_{sc}) \\ &= 4\pi\epsilon A^2 - I(0, T_{sc}) - M_R(T_{sc})(T_{sc} - T_c), \end{aligned} \quad (8.19)$$

where $I(0, T_{sc})$ is the constant $O(1)$ action associated with the homoclinic orbit of the saddle-center bifurcation. Using (8.18) we obtain

$$\begin{aligned} \Delta I &= 4\pi\epsilon A^2 - I(0, T_{sc}) + \epsilon^{4/5} M_R(T_{sc})(3\beta f_T)^{-1/5} \tau_p \\ &\quad - \frac{2}{\beta^{1/3}} \epsilon^{5/6} |M_R(T_{sc})|^{5/6} t_- \zeta \left(\frac{1}{6}, 1 \right). \end{aligned} \quad (8.20)$$

Since the solution passes much closer to the saddle point when the first Painlevé is valid, the change in action is $O(\epsilon^{4/5})$ and larger than usual. The $O(\epsilon)$ term will only be asymptotically significant if the higher order corrections to the other terms are smaller. A_p is determined from connection formulas associated with the first Painlevé requiring τ_p and c_p (given by (8.16)). Equation (8.19) may be preferable since it shows how the change in action is determined by final conditions (T_c).

9. Summary of Crossing Saddle-Center Homoclinic Orbit and an Example

We describe the different kinds of solutions that can occur backwards in time in the case in which the averaged energy is predicted to be zero at the saddle-center bifurcation time ($T_c = T_{sc}$). Solutions consist of strongly nonlinear oscillations that become a large

sequence of nearly saddle-center homoclinic orbits. After this large sequence,

- I. In most cases, the solution passes through the saddle-center homoclinic orbit, reemerging as a strongly nonlinear oscillation resembling the saddle-center homoclinic orbits.
- II. However, for a special class of final conditions in which the energy at a saddle approach is predicted to be unusually small, one saddle approach is described by the non-autonomous first Painlevé transcendent. This first Painlevé transcendent has a finite time singularity forward in time that matches to the first of a series of nearly saddle-center homoclinic orbits. In this case, three things can occur backwards in time depending on the solutions of the first Painlevé transcendent:
 - a. If the first Painlevé approaches the stable center (backwards in time), this involves the transition to small oscillations around the newly created stable center.
 - b. If the first Painlevé approaches the unstable saddle point, this involves the highly unlikely but still possible transition to the unstable saddle point (the two branches of the stable manifold of the unstable saddle point).
 - c. The first Painlevé may also have a finite time singularity backward in time, in which case the solution becomes another nearly saddle-center homoclinic orbit, and the solution will be very similar to case I.

The small band of nearly linear oscillations described by IIa has probability $O(\epsilon^{1/5})$ occurring backwards in time. This band is bounded by IIb, the two branches of the stable manifold of the saddle point, which separate IIa small oscillations from IIc, nearly saddle-center homoclinic orbit. One branch of the stable manifold of the saddle point consists of a large sequence of nearly saddle-center homoclinic orbits, while the other branch is similar but preceded by a single passage around the slowly varying center.

As an example of a slowly varying saddle-center bifurcation, we briefly consider

$$\frac{d^2x}{dt^2} = -(x - 1 + \epsilon t)(x^2 + \epsilon t). \quad (9.1)$$

The leading-order slowly varying equilibria are $x = 1 - \epsilon t$ and $x^2 = -\epsilon t$ so that a saddle center bifurcation occurs at $T_{sc} = \epsilon t_{sc} = 0$, and the bifurcation diagram is as shown in Figure 2. We choose $\epsilon = 10^{-5}$ so that there exists solutions very close to the saddle-center homoclinic orbit, and we numerically integrate. We choose the final energy such that $T_c = T_{sc} = 0$, and we vary the final phase. In Figure 7a, we show a solution consisting of a sequence of nearly saddle-center homoclinic orbits having an autonomous transition between positive and negative energies. Figure 7b shows a solution that undergoes a nonautonomous (first Painlevé) transition between a sequence of nearly saddle-center homoclinic orbits and small oscillations around the slowly varying center $x \sim -\sqrt{-\epsilon t}$ for $\epsilon t < 0$. In Figures 7a and 7b, we also illustrate the projection of the solutions in the two-dimensional $(x, \frac{dx}{dt})$ phase space, verifying that the solutions are nearly saddle-center homoclinic orbits.

Appendix: Analytic Continuation of the Generalized Riemann Zeta Function

The saddle times t_i for nearly saddle-center homoclinic orbits ($T_c = T_{sc}$) can be obtained by summing the difference equation (6.3). Since the sum is divergent, we are interested

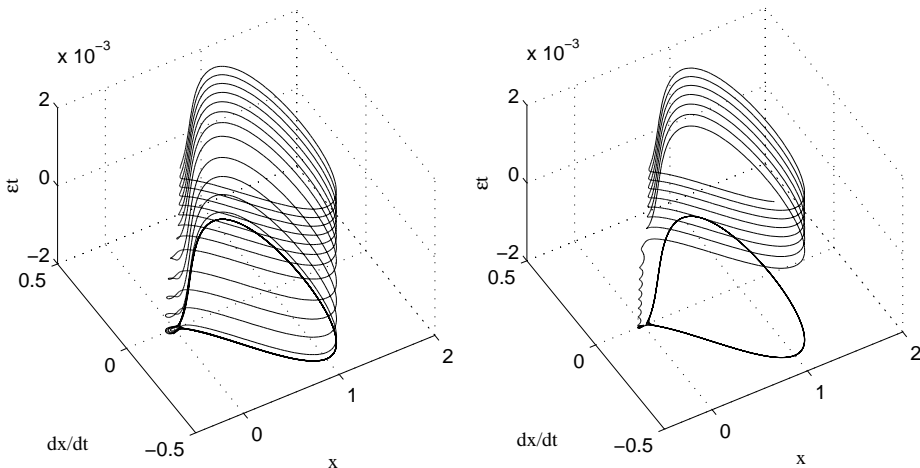


Fig. 7. Autonomous (a) transition between sequences of nearly saddle-center homoclinic orbits with positive and negative energies. Nonautonomous (b) transition (first Painlevé) between small oscillations around the center and a sequence of nearly saddle-center homoclinic orbits.

instead in the asymptotic expansion of the saddle times as $i \rightarrow \mp\infty$. Similar convergent sums can be expressed in terms of the generalized Riemann zeta function. We will follow the well-known [8] ideas of analytic continuation as first described by Riemann and apply it to the generalized Riemann zeta function [5]. We will show that the regularization of our divergent sum equals the analytic continuation of the corresponding generalized Riemann zeta function. The particular divergent sum of interest to us follows from (6.3)

$$R_m(a) = \sum_{n=0}^{m-1} (a+n)^{-1/6} \quad (\text{A.1})$$

with $a > 0$. The leading-order term in the asymptotic expansion for large m of (A.1) may be obtained by elementary methods, $R_m(a) \sim \frac{6}{5}m^{5/6} + k$, where we wish to determine the more difficult constant k . An integral representation of the corresponding infinite series is usually obtained by introducing an infinite geometric series with the gamma function $\Gamma(\frac{1}{6}) = (a+n)^{1/6} \int_0^\infty x^{-5/6} e^{-(a+n)x} dx$ requiring $a+n > 0$. Here, we must instead use a finite geometric series

$$\Gamma\left(\frac{1}{6}\right) R_m(a) = \int_0^\infty e^{-ax} \frac{x^{-5/6}}{1 - e^{-x}} (1 - e^{-mx}) dx. \quad (\text{A.2})$$

The limit as $m \rightarrow \infty$ of (A.2) does not exist because of the nonintegrable singularity $x^{-5/6} \frac{1}{x}$ at $x = 0$, which we remove in the following way: $\Gamma(\frac{1}{6}) R_m(a) = \int_0^\infty x^{-11/6} (1 -$

$e^{-mx}) dx + \int_0^\infty (e^{-ax} \frac{x^{-5/6}}{1-e^{-x}} - x^{-11/6})(1 - e^{-mx}) dx$. The first integral can be easily evaluated by letting $u = mx$ and integrating by parts, while the second integral has a limit as $m \rightarrow \infty$:

$$R_m(a) \sim \frac{6}{5}m^{5/6} + \frac{1}{\Gamma(\frac{1}{6})} \int_0^\infty \left(e^{-ax} \frac{x^{-5/6}}{1-e^{-x}} - x^{-11/6} \right) dx. \quad (\text{A.3})$$

We show that this regularized integral in (A.3) is related to the analytic continuation of the generalized Riemann-zeta function. We introduce the function of the complex variable z , $F(z) = \frac{1}{\Gamma(\frac{1}{6})}(-z)^{1/6}[\frac{e^{-az}}{z(1-e^{-z})} - \frac{1}{z^2}]$, analytic in the cut plane to be described, where in the usual way $(-z)^{1/6} = e^{\frac{1}{6}\log(-z)} = |z|^{1/6}e^{\frac{i}{6}\arg(-z)}$. We integrate along Riemann's contour C , starting along the real positive axis x from $+\infty$, circling the origin in the positive (counterclockwise) direction, and returning to $+\infty$ along the positive real axis. In this way the contribution around the singularity $(-z)^{1/6-1}$ vanishes (since it is less than a pole) $\int_C F(z) dz = \frac{1}{\Gamma(\frac{1}{6})}(e^{i\pi/6} - e^{-i\pi/6}) \int_0^\infty (e^{-ax} \frac{x^{-5/6}}{1-e^{-x}} - x^{-11/6}) dx$. Since $\int_C (-z)^{1/6} \frac{1}{z^2} dz = 0$, because its antiderivative vanishes at the endpoints at infinity, it follows that

$$R_m(a) \sim \frac{6}{5}m^{5/6} + \frac{1}{\Gamma(\frac{1}{6})} \frac{1}{e^{i\pi/6} - e^{-i\pi/6}} \int_C e^{-az} \frac{(-z)^{1/6}}{z(1-e^{-z})} dz. \quad (\text{A.4})$$

The analytic continuation of the generalized Riemann zeta function is defined [5] by

$$\zeta\left(\frac{1}{6}, a\right) = \frac{1}{2\pi i} \Gamma\left(\frac{5}{6}\right) \int_C e^{-az} \frac{(-z)^{1/6}}{z(1-e^{-z})} dz. \quad (\text{A.5})$$

From the reflection formula for gamma functions, $\Gamma(z)\Gamma(1-z) = \frac{\pi}{\sin \pi z}$, we have $\Gamma(\frac{1}{6})\Gamma(\frac{5}{6}) = \frac{\pi}{\sin(\pi/6)}$. Thus,

$$R_m(a) \sim \frac{6}{5}m^{5/6} + \zeta\left(\frac{1}{6}, a\right). \quad (\text{A.6})$$

The generalized Riemann zeta function is usually defined [5] and [8] by a convergent series and its equivalent integral representation. The analytic continuation is introduced to define the generalized Riemann zeta function when neither the infinite series nor its usual integral representation exists. Here, we have derived the important formula (A.6) that the regularized sum $(\lim_{m \rightarrow \infty} R_m(a) - \frac{6}{5}m^{5/6})$ equals the analytic continuation of the divergent sum.

References

- [1] Arnold, V. I., Kozlov, V. V., and Neishtadt, A. I., *Mathematical Aspects of Classical and Celestial Mechanics, Dynamical Systems III*, Springer-Verlag, New York, 1988.
- [2] Bourland, F. J., and Haberman, R., Separatrix crossing: Time-invariant potentials with dissipation, *SIAM J. Appl. Math.*, **50** (1990), pp. 1716–1744.
- [3] Bourland, F. J., Haberman, R., and Kath, W. L., Averaging methods for the phase shift of arbitrarily perturbed strongly nonlinear oscillators with an application to capture, *SIAM J. Appl. Math.*, **51** (1991), pp. 1150–1167.
- [4] Bourland, F. J., and Haberman, R., Connection across a separatrix with dissipation, *Stud. Appl. Math.*, **91** (1994), pp. 95–124.
- [5] Carrier, G. F., Krook, M., and Pearson, C. E., *Functions of a Complex Variable*, McGraw-Hill, New York, 1966, pp. 192–194.
- [6] Cary, J. R., Escande, D. F., and Tennyson, J. L., Adiabatic-invariant change due to separatrix crossing, *Phys. Rev. A*, **34** (1986), pp. 4256–4275.
- [7] Cary, J. R., and Skodje, R. T., Phase change between separatrix crossings, *Physica D*, **36** (1989), pp. 287–316.
- [8] Edwards, H. M., *Riemann's Zeta Function*, Academic Press, New York, 1974, pp. 9–11.
- [9] Fokas, A. S., Mugan, U., and Zhou, X., On the solvability of Painlevé I, III and V, *Inverse Problems*, **8** (1992), pp. 757–785.
- [10] Golubitsky, M., and Schaeffer, D. G., *Singularities and Groups in Bifurcation Theory, Vol. 1*, Springer-Verlag, New York, 1985.
- [11] Golubitsky, M., Stewart, I., and Schaeffer, D. G., *Singularities and Groups in Bifurcation Theory, Vol. 2*, Springer-Verlag, New York, 1988.
- [12] Guckenheimer, J., and Holmes, P. J., *Nonlinear Oscillations, Dynamical Systems, and Bifurcations of Vector Fields*, Springer-Verlag, New York, 1983.
- [13] Haberman, R., Slowly varying jump and transition phenomena associated with algebraic bifurcation problems, *SIAM J. Appl. Math.*, **37** (1979), pp. 69–109.
- [14] Henrard, J. The adiabatic invariant in classical mechanics, in *Dynamics Reported Expositions in Dynamical Systems New Series: Volume 2*, eds. C. K. R. T. Jones, U. Kirchgraber, H. O. Walther, Springer-Verlag, New York, 1993, pp. 117–235.
- [15] Ince, E. L., *Ordinary Differential Equations*, Dover, New York, 1956.
- [16] Its, A. R., and Novokshenov, V. Y., The Isomonodromic Deformation Method in the Theory of Painlevé Equations, in *Lecture Notes in Mathematics Vol. 1191*, Springer-Verlag, New York, 1986.
- [17] Kapaev, A. A., Asymptotics of solutions of the Painlevé equation of the first kind, *Diff. Eq.* **24** (1988), pp. 1107–1115 [*Diff. Urav.*, **24** (1988), pp. 1684–1695].
- [18] Lebovitz, N. R., and Schaar, R. J., Exchange of stabilities in autonomous systems, *Stud. Appl. Math.*, **54** (1975), pp. 229–260.
- [19] Lebovitz, N. R., and Schaar, R. J., Exchange of stabilities in autonomous systems—II. Vertical bifurcation, *Stud. Appl. Math.*, **56** (1977), pp. 1–50.
- [20] Mareé, G. J. M., Slow passage through a pitchfork bifurcation, *SIAM J. Appl. Math.*, **56** (1996), pp. 889–918.
- [21] Neishtadt, A. I., Passage through a separatrix in a resonance problem with a slowly varying parameter, *Prikl. Mat. Mekh.*, **39** (1975), pp. 621–622 [*J. Appl. Math. Mech.*, **39** (1975), pp. 594–605].
- [22] Neishtadt, A. I., Change of an adiabatic invariant at a separatrix, *Fiz. Plazmy*, **12** (1986), pp. 992–1001 [*J. Plasma Phys.*, **12** (1986), pp. 568–573].
- [23] Neishtadt, A. I., Persistence of stability loss for dynamical bifurcations. I, *Diff. Urav.*, **23** (1987), pp. 2060–2067 [*Diff. Eq.*, **23** (1987), pp. 1385–1391].
- [24] Neishtadt, A. I., Persistence of stability loss for dynamical bifurcations. II, *Diff. Urav.*, **24** (1988), pp. 226–233 [*Diff. Eq.*, **24** (1988), pp. 171–176].

- [25] Neishtadt, A. I., Vainshtein, D. L., and Vasiliev, A. A., Chaotic advection in a cubic Stokes flow, *Physica D*, **111** (1998), pp. 227–242.
- [26] Sanders, J. A., and Verhulst, F., *Averaging Methods in Nonlinear Dynamical Systems*, Springer-Verlag, New York, 1985.
- [27] Vainshtein, D. L., Vasiliev, A. A., and Neishtadt, A. I., Changes in the adiabatic invariant and streamline chaos in confined incompressible Stokes flow, *Chaos*, **6** (1996), pp. 67–77.